Journal of Power Sources 189 (2009) 95–100

Contents lists available at ScienceDirect

Journal of Power Sources

journal homepage: www.elsevier.com/locate/jpowsour

Preparation of manganese oxide with high density by decomposition of $MnCO_3$ and its application to synthesis of $LiMn_2O_4$

Hua-jun Guo*, Xin-hai Li, Zhi-xing Wang, Wen-jie Peng, Xuan Cao, Hui-feng Li

School of Metallurgical Science and Engineering, Central South University, Changsha 410083, China

ARTICLE INFO

Article history:
Received 28 June 2008
Received in revised form 23 October 2008
Accepted 24 October 2008
Available online 5 November 2008

Keywords:
Lithium ion batteries
Cathode
Manganese oxide
$LiMn_2O_4$
Decompose

ABSTRACT

Manganese oxide with high tap density was prepared by decomposition of spherical manganese carbonate, and then $LiMn_2O_4$ cathode materials were synthesized by solid-state reaction between the manganese oxide and lithium carbonate. Structure and properties of the samples were determined by X-ray diffraction, Brunauer–Emmer–Teller surface area analysis, scanning electron microscope and electrochemical measurements. With increase of the decomposition temperature from 350 °C to 900 °C, the tap density of the manganese oxide rises from 0.91 g cm^{-3} to 2.06 g cm^{-3}. Compared with the $LiMn_2O_4$ cathode made from chemical manganese dioxide or electrolytic manganese dioxide, the $LiMn_2O_4$ made from manganese oxide of this work has a larger tap density (2.53 g cm^{-3}), and better electrochemical performances with an initial discharge capacity of 117 mAh g^{-1}, a capacity retention of 93.5% at the 15th cycle and an irreversible capacity loss of 2.24% after storage at room temperature for 28 days.

1. Introduction

Advanced rechargeable lithium ion batteries are attractive for use in consumer electronic and electric vehicle application and have developed rapidly worldwide. $LiMn_2O_4$ spinel is a prospective cathode of lithium ion batteries because of a favorable combination of electrochemical performances, cost, safety and non-toxicity [1].

The capacity fading upon cycling at elevated temperature and irreversible capacity loss during storage are the great problems for the application of $LiMn_2O_4$ [2,3]. Reasons such as manganese dissolution, electrolyte decomposition, Jahn-Teller effect, particle disruption and lattice instability have been proposed for the capacity loss [4,5]. Many efforts have been devoted to improving the elevated temperature performance by substituting O with F [6,7], coating the spinel with Li_2O, B_2O_3, Al_2O_3, MgO, $LiCoO_2$ [1,3,8,9], and doping with metal ions such as Co^{3+}, Cr^{3+}, Al^{3+} and Mg^{2+} [10–14]. However, despite the improvement of cycle stability at elevated temperature, $LiMn_2O_4$ has still suffered from significant capacity fading during storage.

Improvement on energy density is another challenge for application of $LiMn_2O_4$. Compared with the commercial $LiCoO_2$ cathode, $LiMn_2O_4$ cathode has much lower energy density. It can be attributed to $LiMn_2O_4$ spinel's much smaller impacted density after electrode rolling as well as the lower specific capacity. Impacted density above 4.0 g cm^{-3} has been used for the fabrication of $LiCoO_2$ electrode in industry, while that for the $LiMn_2O_4$ electrode is just 2.8 g cm^{-3} approximately. So the energy density by volume for lithium ion battery with $LiMn_2O_4$ cathode is only 70% of that with $LiCoO_2$ cathode.

It is well known that the physical properties and the electrochemical performances of cathodes depend upon the synthesis method and the properties of precursors employed [15–18]. Chemical manganese dioxide (chemically prepared manganese dioxide, CMD) and electrolytic manganese dioxide (manganese dioxide prepared by electrochemical methods, EMD) have been widely used as manganese compound precursors for synthesis of $LiMn_2O_4$ powders. However, the commercial CMD and EMD precursors usually have disordered appearance, low density and large surface area, and they are not suitable for preparation of $LiMn_2O_4$ powder with large density. Therefore, the present work aims to develop a new manganese oxide precursor with high tap density, low surface area and good morphology by decomposition of spherical manganese carbonate, and then apply it to synthesis of $LiMn_2O_4$ spinel cathode with large tap density and improved storage performance.

2. Experimental

Thermal gravimetric analysis (TGA) of spherical manganese carbonate was done on a Mettler Toledo TGA/SDTA851e thermal gravimetric analyzer. The sample was held in a Corundum Pan and heated to 800 °C at 10 °C min^{-1} in air.

* Corresponding author. Tel.: +86 731 8836633.
E-mail address: ghj.csu@163.com (H.-j. Guo).

0378-7753/$ – see front matter © 2008 Elsevier B.V. All rights reserved.
doi:10.1016/j.jpowsour.2008.10.099

Manganese oxide was prepared by decomposition of spherical manganese carbonate at different temperatures for 4 h in air. The heating rate of the samples was 10 °C min^{-1}.

$LiMn_2O_4$ cathode materials were synthesized by solid-state reaction between the manganese oxide and lithium carbonate. The manganese oxide (or CMD, EMD) and Li_2CO_3 were mixed in stoichiometric proportion, ground, and then calcined at 750 °C for 24 h in air. The cooling rate of the powder was 2 °C min^{-1}.

Powder X-ray diffraction (XRD) measurements were conducted using a Rigaku diffractometer. Scanning electron micrographs (SEM) were obtained with a JEOL JSM-5600LV spectrometer. Brunauer–Emmer–Teller (BET) surface area measurements were performed using a Quantacgrome monosorb surface area analyzer. Tap density of the powders was characterized as follows. The powder (15 g approximately) was added into a 20-ml glass measuring cylinder, then the measuring cylinder was lifted at the height of 10 cm and fall onto a ebonite board of 2 cm thickness for 200 times. The tap density was calculated according to the mass and the last volume of the powder.

The $LiMn_2O_4$ spinel, acetylene black and poly-vinylidene difluoride (PVDF) were mixed in *N*-methyl-2-pyrrolidone in a weight ratio of 8:1:1. The $LiMn_2O_4$ cathode was prepared by spreading the above mixture on aluminum foil. Charge–discharge tests of the $LiMn_2O_4$ spinels were performed in the coin cells with $LiMn_2O_4$ cathode and lithium anode. A UP 3025 porous membrane of 25 μm thickness was used as a separator. The electrolyte was 1 mol L^{-1} $LiPF_6$ dissolved in a mixture of ethylene carbonate (EC), dimethyl carbonate (DMC) and methyl-ethyl carbonate (EMC) with a volume ratio of 1:1:1. The charge–discharge characteristics and cycling performance of coin cells were investigated in the voltage range of 3.0–4.2 V at a current density of 25 mA g^{-1}.

Prismatic 204465-type cells (thickness: 20 mm; width: 44 mm; height: 65 mm) were fabricated with $LiMn_2O_4$ as the positive electrodes, an artificial graphite as the negative electrodes and 1 mol L^{-1} LiPF6-EC/DMC/EMC electrolyte. The initial discharge capacity of the prismatic 204465-type cells was determined by charge–discharge in the voltage range of 3.0–4.2 V at a current density of 50 mA g^{-1}, then the cells with state of charge (SOC) of 50% were stored at room temperature for 28 days. After the storage, the cells were charge–discharged for three cycles at a current density of 50 mA g^{-1}, and irreversible capacity loss of the cells during the storage (the difference of initial discharge capacity and the stable discharge capacity after the storage) was obtained.

3. Results and discussion

3.1. Characterization of spherical manganese carbonate

Fig. 1 shows SEM of spherical manganese carbonate. The powders consist of aggregate particles. The primary particles of the manganese carbonate are spherical in shape. The primary particle size lies in 0.5–5 μm. Owing to the well-developed spherical micrographs, the sample has a large tap density of 1.54 g cm^{-3}.

Fig. 2 shows the TG analysis profile of the manganese carbonate. The first obvious weight loss (7.1%) observed at around 80 °C is due to dehydration of the powder. The second large weight loss (17.9%) occurs in the temperature of 320–435 °C, and it can be attributed to the decomposition of manganese carbonate. In the temperature range of 435–750 °C, the weight of the sample keeps constant. A light weight loss can be detected when the temperature is above 750 °C, and it may result from the deoxidation of the manganese oxide.

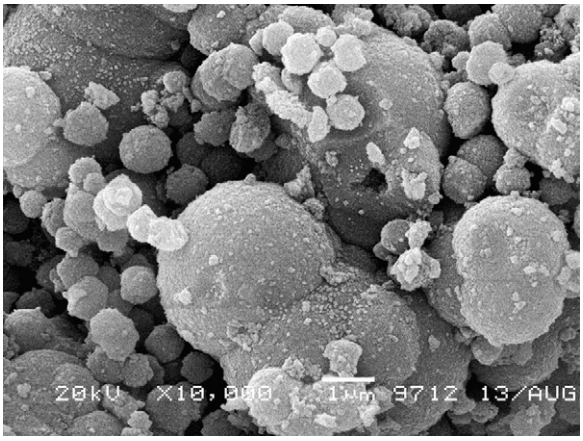

Fig. 1. SEM image of spherical manganese carbonate.

3.2. Properties of manganese oxide

According to the results of TG analysis, a temperature range of 350–900 °C was determined to decompose spherical manganese carbonate. Manganese oxide was obtained by decomposition of the manganese carbonate powder at different temperatures for 4 h. Fig. 3 shows XRD patterns of the manganese oxide. The XRD patterns were identified as Mn_2O_3 (JCPDS No. 71-0636), but the XRD patterns for the sample obtained at 350 °C shows a low intensity and broad diffraction peaks, suggesting it has poor crystallinity. As the decomposition temperature rises, the diffraction peaks become intense and sharp, indicating the crystallinity increases. However, a little secondary phase assigned to Mn_3O_4 (JCPDS No. 24-0734) was discovered in the XRD patterns for the samples decomposed at 800 °C and 900 °C. It is due to deoxidation of Mn_2O_3 at high temperature, which is consistent with the results of TG analysis shown in Fig. 2.

Fig. 4 shows micrographs of the manganese oxide decomposed at different temperatures for 4 h. Aggregation phenomenon is observed for each sample. The sample obtained at 600 °C consists of spherical primary particles, which is similar to the manganese carbonate precursor. But the spherical morphology of the primary particles is destroyed and new primary particles with tight and smooth surface is formed when the decomposition temperature is above 700 °C. A primary particle size range of 0.5–2 μm was observed for the manganese oxide sample decomposed at 600 °C. The sample obtained at 700 °C shows the smallest primary particle size which lies in 0.2–0.5 μm. The primary particle grows with increasing decomposition temperature from 700 °C to 900 °C. The

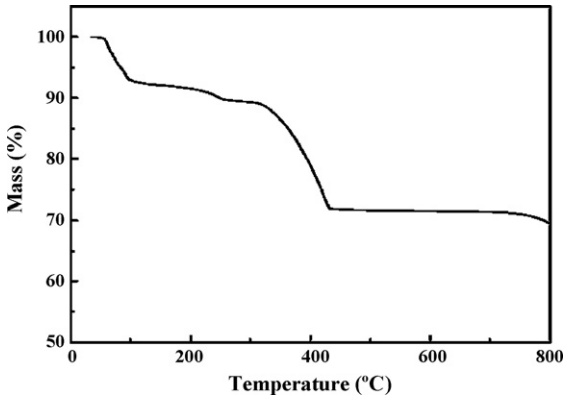

Fig. 2. TG analysis profile of spherical manganese carbonate.

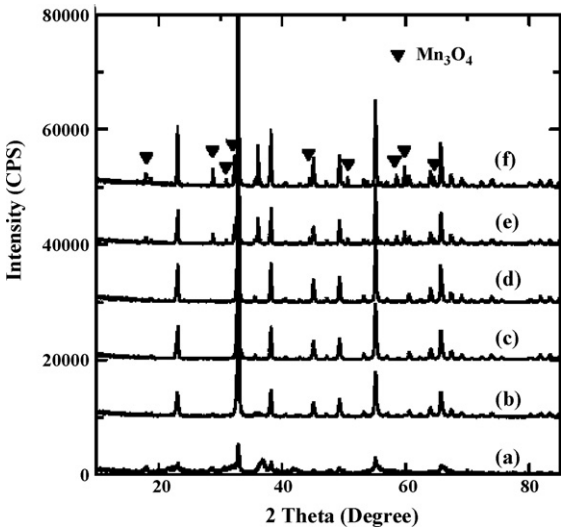

Fig. 3. XRD patterns of manganese oxide decomposed at different temperatures. (a) 350 °C; (b) 500 °C; (c) 600 °C; (d) 700 °C; (e) 800 °C and (f) 900 °C.

sample decomposed at 900 °C consists of large and uniform primary particles with diameter of around 1 μm.

Tap density is an important parameter for powder electrode active materials. It refers to the apparent powder density obtained under stated conditions of vibration or tapping. In this work, the tap density of manganese oxide was measured by tapping a 20-ml measuring cylinder filled with 15 g (approximately) powder on an ebonite board for 200 times, and the results were listed in Table 1. As the decomposition temperature rises from 350 °C to 900 °C, the tap density of manganese oxide increases, and the manganese oxide decomposed at 900 °C for 4 h has the largest tap density of 2.06 g cm^{-3}. A sharp rise of 40% in tap density occurs in the temperature range of 700–750 °C, though the big difference in appearance of the primary particles was seen between 600 °C and 700 °C according to the SEM observation. It can be attributed to the combined effects of appearance and particle size on the tap density. The particles of the sample obtained at 700 °C have tighter and smoother surface than those at 600 °C, but they have a much smaller size. As a result, the tap density does not increase dramatically between 600 °C and 700 °C. When the decomposition temperature is above 750 °C, the tap density of the manganese oxide is greatly improved due to the increase in particle size.

Table 1
Tap density for manganese oxide decomposed at different temperatures for 4 h.

Temp. (°C)	Tap density (g cm^{-3})
350	0.91
500	1.01
600	1.08
700	1.28
750	1.79
800	1.84
900	2.06

As a precursor of $LiMn_2O_4$ spinel, the properties of manganese oxide play important roles on structure and performances of the spinels. With relatively good combination of large tap density and small particle size which is favorable for the solid-state reaction, the

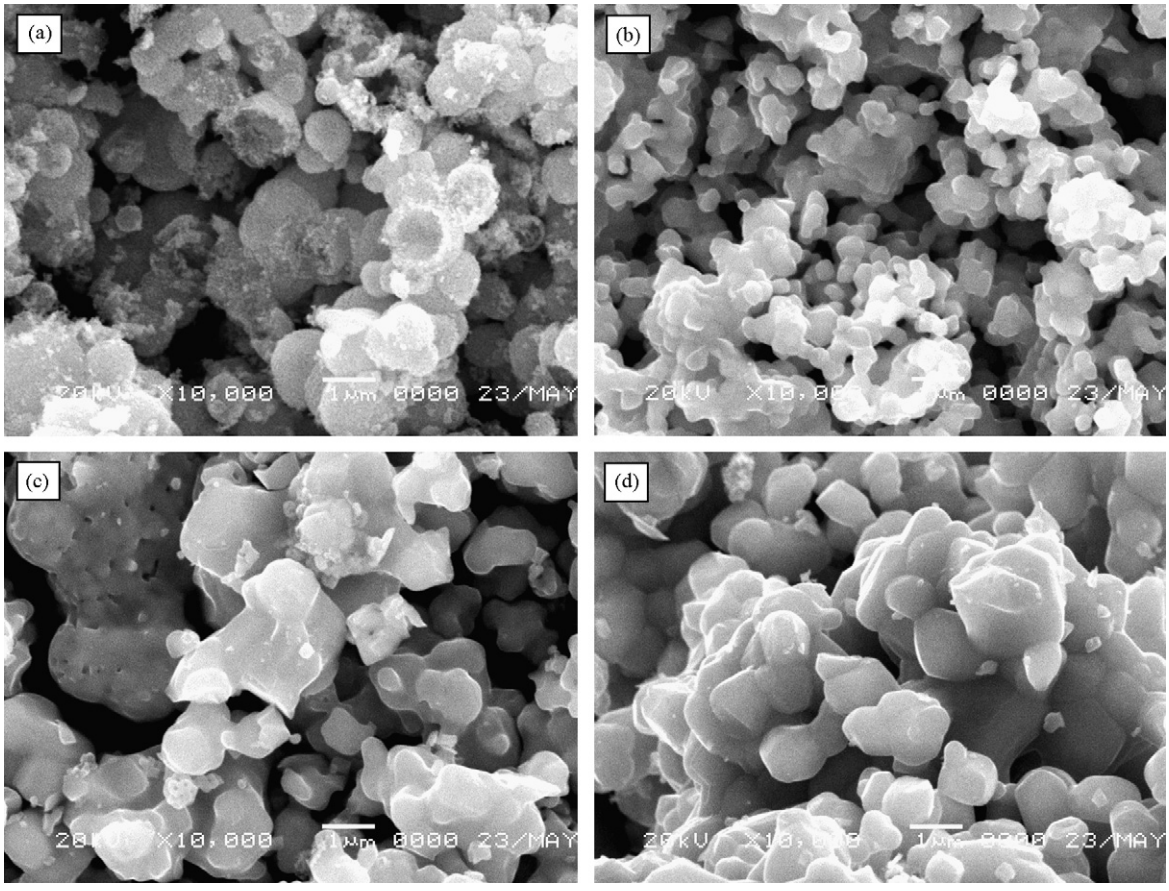

Fig. 4. SEM images of manganese oxide decomposed at different temperatures. (a) 600 °C; (b) 700 °C; (c) 800 °C and (d) 900 °C.

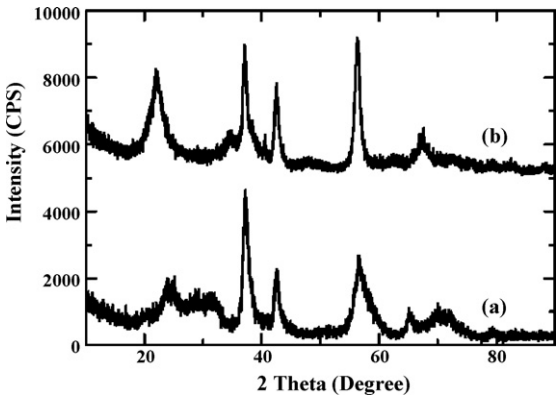

Fig. 5. XRD patterns of (a) chemical manganese dioxide and (b) electrolytic manganese dioxide.

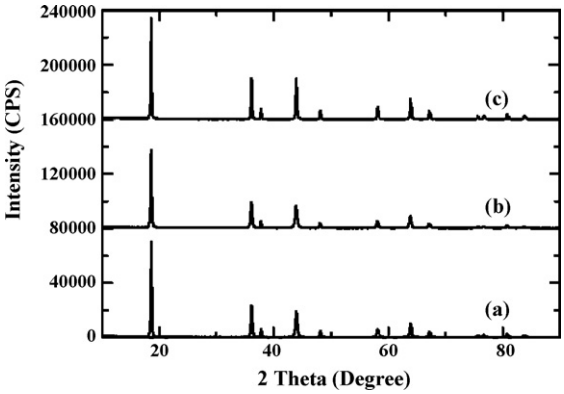

Fig. 7. XRD patterns of $LiMn_2O_4$ spinels made from different precursors. (a) $LiMn_2O_4$-C; (b) $LiMn_2O_4$-E and (c) $LiMn_2O_4$-W.

manganese oxide obtained at 800 °C was chosen as the precursor and applied to synthesis of $LiMn_2O_4$ spinel, and commercial CMD and EMD were used as precursors of $LiMn_2O_4$ spinel for comparison.

Fig. 5 shows XRD patterns of CMD and EMD. All the peaks for CMD were indexed on the €-MnO_2 (JCPDS No. 30-0820), and those for EMD on the γ-MnO_2 (JCPDS No. 14-0644). The XRD patterns for both samples show low intensity and broadening of the XRD peaks, suggesting the samples have low crystallinity.

Fig. 6 shows the micrographs of CMD and EMD. Both samples consist of primary particles with disordered appearance, and there are many tiny particles observed on the surface. As a result, the tap density of CMD and EMD is 1.56 g cm^{-3} and 1.77 g cm^{-3}, respectively, which is lower than that of the manganese oxide prepared by decomposition of spherical manganese carbonate at 800 °C for 4 h.

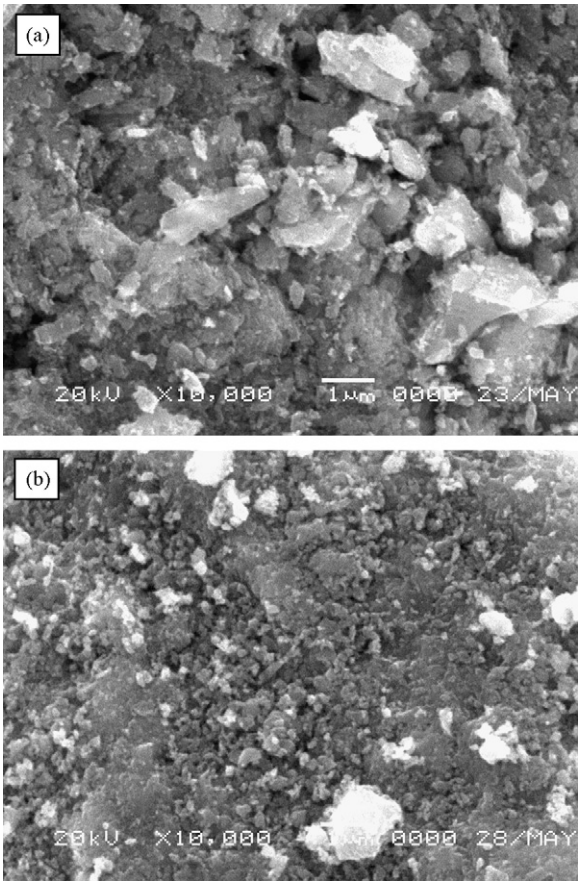

Fig. 6. SEM images of (a) chemical manganese dioxide and (b) electrolytic manganese dioxide.

3.3. Performances of $LiMn_2O_4$ spinels

$LiMn_2O_4$ spinels were synthesized using CMD, EMD and manganese oxide of this work as manganese compound precursors, which were labeled as $LiMn_2O_4$-C, $LiMn_2O_4$-E and $LiMn_2O_4$-W, respectively.

Fig. 7 shows the XRD patterns of $LiMn_2O_4$ spinels made from different precursors. All the XRD patterns were identified as pure Mn-spinel phase (a space group *Fd3m*). The lattice parameter calculated from the XRD pattern for $LiMn_2O_4$-C, $LiMn_2O_4$-E and $LiMn_2O_4$-W is 8.2338 Å, 8.2392 Å and 8.2316 Å, respectively. The XRD pattern for the sample $LiMn_2O_4$-W shows the sharpest and intensest diffraction peaks, which suggests that the $LiMn_2O_4$ made from manganese oxide of this work ($LiMn_2O_4$-W) has the best crystallinity.

Fig. 8 shows the SEM images of $LiMn_2O_4$ spinels made from different precursors. The $LiMn_2O_4$ powder made from CMD consists of disordered primary particles whose size lies in 0.1–0.8 μm, and the primary particles aggregate loosely. The $LiMn_2O_4$ powder made from EMD also consists of disordered primary particles, and there are many tiny particles observed on the surface of the sample. While the $LiMn_2O_4$ spinel made from manganese oxide of this work exhibits a tight surface and the morphology of the primary particles is octahedral in shape.

As results of difference in the structure and morphology, the $LiMn_2O_4$ spinels made from various precursors present large difference on the tap density and specific surface area. The results of tap density and BET specific area measurements for $LiMn_2O_4$ samples are listed in Table 2. Among the samples, the $LiMn_2O_4$ made from manganese oxide of this work ($LiMn_2O_4$-W) presents the largest tap density of 2.53 g cm^{-3} and the lowest specific sur-

Table 2
Tap density and BET specific surface area for $LiMn_2O_4$ made from different precursors.

Sample	$LiMn_2O_4$-C	$LiMn_2O_4$-E	$LiMn_2O_4$-W
Precursors adopted	CMD	EMD	Manganese oxide of this work
Tap density (g cm^{-3})	2.05	2.08	2.53
BET specific surface area (m^2 g^{-1})	2.98	1.20	0.60

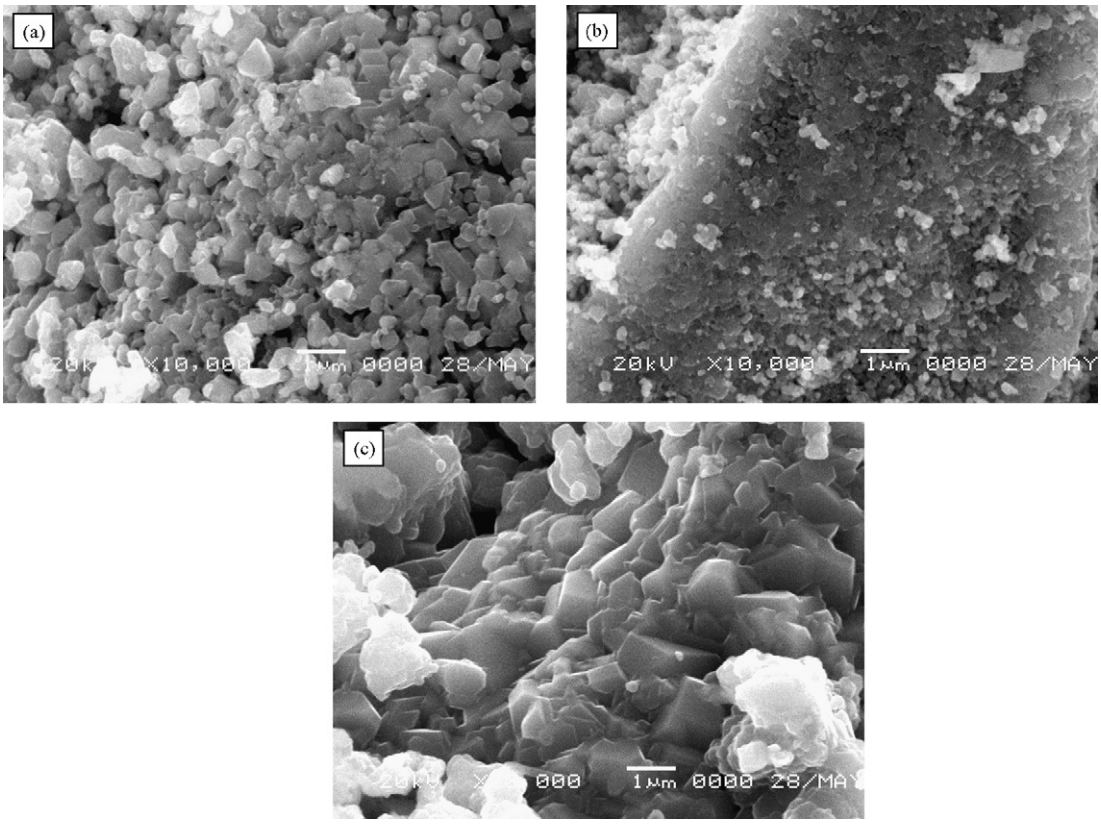

Fig. 8. SEM images of $LiMn_2O_4$ spinels made from different precursors. (a) $LiMn_2O_4$-C; (b) $LiMn_2O_4$-E and (c) $LiMn_2O_4$-W.

face area of 0.60 $m^2\,g^{-1}$. It is due to the good morphology as well as large tap density of the manganese oxide decomposed from spherical manganese carbonate. The tap density of the $LiMn_2O_4$-W is also much larger than that of spherical $Li_{1.05}M_{0.05}Mn_{1.9}O_4$ (M = Mn, Ni, Mg, Al) obtained by co-precipitation synthesis (1.85–2.05 g cm^{-3} approximately) and that of sphereical $LiMn_2O_4$ synthesized by a combination of spray pyrolysis and drying method (1.32 g cm^{-3}) reported in the related literature [17,18].

The specific capacity and cycling performance of the $LiMn_2O_4$ spinels were measured in coin cells with $LiMn_2O_4$ cathode and lithium anode, which is shown in Fig. 9. The $LiMn_2O_4$-C cathode and $LiMn_2O_4$-E cathode deliver the same initial discharge capacity of 113 mAh g^{-1} (76.3% of the theoretical value), while the $LiMn_2O_4$ cathode made from manganese oxide of this work shows the largest initial discharge capacity of 117 mAh g^{-1} (79.1% of the theoretical value). After charge–discharged for 15 cycles, a capacity retention of 92.3%, 93.1% and 93.5% is observed for the $LiMn_2O_4$-C, $LiMn_2O_4$-E and $LiMn_2O_4$-W cathode, respectively, suggesting that the $LiMn_2O_4$-W cathode has the best cycling performance.

In order to investigate the effects of precursors on performances of the practical lithium ion cells, prismatic 204465-type cells were fabricated with $LiMn_2O_4$ cathodes made from different precursors. The maximum impacted density of $LiMn_2O_4$-C, $LiMn_2O_4$-E and $LiMn_2O_4$-W is 2.72 g cm^{-3}, 2.85 g cm^{-3} and 3.10 g cm^{-3}, respectively. The cells were designed to have same degree of tightness and mass ratio of cathode to anode. After charged–discharged for three cycles, the cells with 50% SOC were stored at room temperature for 28 days. The discharge curves before storage and those after storage at a current density of 50 mA g^{-1} are shown in Fig. 10. The cell with $LiMn_2O_4$-C cathode and that with $LiMn_2O_4$-E cathode show initial discharge capacity of 3.96 Ah and 4.07 Ah, respectively, while the cell with $LiMn_2O_4$-W cathode has a much higher initial dis-

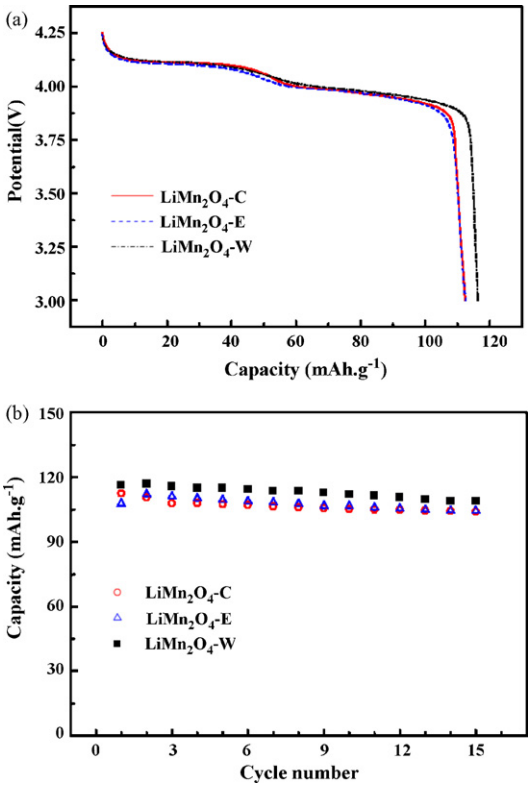

Fig. 9. Electrochemical performances of $LiMn_2O_4$ made from different precursors at a current density of 25 mA g^{-1}. (a) Initial discharge voltage curves and (b) cycling performance curves.

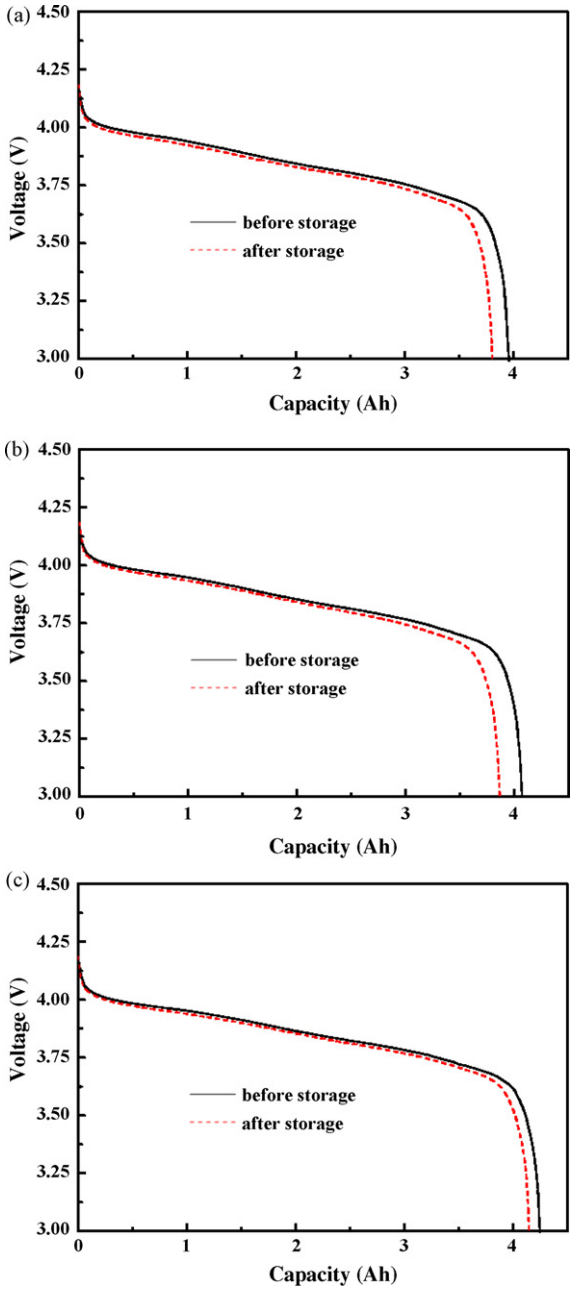

Fig. 10. Storage performance of 204465-type cells with different $LiMn_2O_4$ cathodes. (a) $LiMn_2O_4$-C; (b) $LiMn_2O_4$-E and (c) $LiMn_2O_4$-W.

charge capacity of 4.25 Ah. It can be attributed to the higher specific capacity and larger tap density of the $LiMn_2O_4$ spinel made from manganese oxide of this work, which results in a large impacted density for the positive electrode. Being stored for 28 days at room temperature, then charge–discharged for three cycles, the cell with $LiMn_2O_4$-C cathode and that with $LiMn_2O_4$-E cathode present discharge capacity of 3.81 Ah and 3.87 Ah, respectively, suggesting an irreversible capacity loss of 3.79% and 4.80% occurs during the storage. While the cell with $LiMn_2O_4$ cathode made from manganese oxide precursor delivers a discharge capacity of 4.15 Ah after the storage, and the irreversible capacity loss is reduced to 2.24%. The improvement on the storage performance may be due to the well developed primary particles, tight particle surface and low specific surface area, which can depress the undesired reactions during the storage.

4. Conclusions

Manganese oxide was obtained by decomposition of spherical manganese carbonate at different temperatures for 4 h. The products were identified as Mn_2O_3. As decomposition temperature rises, the crystallinity and tap density of the manganese oxide increases, but a little secondary phase assigned to Mn_3O_4 is formed when the decomposition temperature is above 800 °C. The manganese oxide decomposed from spherical manganese carbonate at 900 °C for 4 h has a large tap density of 2.06 g cm^{-3}.

Compared with the $LiMn_2O_4$ cathode made from commercial CMD or EMD, the $LiMn_2O_4$ made from manganese oxide of this work has a larger tap density and better electrochemical performances with a tap density of 2.53 g cm^{-3}, initial discharge capacity of 117 mAh g^{-1}, a capacity retention of 93.5% at the 15th cycle, and an irreversible capacity loss of 2.24% after storage at room temperature for 28 days.

The results show that the manganese oxide prepared by decomposition of spherical manganese carbonate has attractive potential for using as precursor of $LiMn_2O_4$ cathode.

Acknowledgements

The financial support by the National Basic Research Program of China (2007CB613607) and the support from Hunan Shanshan Advanced Material Co., Ltd. are acknowledged.

References

[1] L.J. Fu, H. Liu, C. Li, Y.P. Wu, E. Rahm, R. Holze, H.Q. Wu, Solid State Sci. 8 (2006) 113.
[2] X. Wang, Y. Yagi, Y.S. Lee, M. Yoshio, Y. Xia, T. Sakai, J. Power Sources 97–98 (2001) 427.
[3] C.W. Lee, H.S. Kim, S.I. Moon, Mater. Sci. Eng. B 123 (2005) 234.
[4] A.D. Pasquier, A. Blyr, A. Cressent, C. Lenain, G. Amatucci, J.M. Taraseon, J. Power Sources 81–82 (1999) 54.
[5] T. Aoshima, K. Okahara, C. Kiyohara, K. Shizuka, J. Power Sources 97–98 (2001) 377.
[6] Y.J. Kang, J.H. Kim, Y.K. Sun, J. Power Sources 146 (2005) 237–240.
[7] G.G. Amatucci, N. Pereira, T. Zheng, J. Electrochem. Soc. 148 (2001) A171.
[8] S.B. Park, H.C. Shin, W.G. Lee, W.H. Cho, H. Jang, J. Power Sources 180 (2008) 597.
[9] Z. Liu, H. Wang, L. Fang, J.Y. Lee, L.M. Gan, J. Power Sources 104 (2002) 101.
[10] Y.S. Lee, K. Naoki, Y. Masaki, J. Power Sources 96 (2001) 376.
[11] N. Hayashi, H. Ikuta, M. Wakihara, J. Electrochem. Soc. 146 (1999) 1351.
[12] R. Thirunakaran, K.T. Kim, Y.M. Kang, J.Y. Lee, Mater. Res. Bull. 40 (2005) 177.
[13] M. Takahashi, T. Yoshida, A. Ichikawa, K. Kitoh, H. Katsukawa, Q. Zhang, M. Yoshio, Electrochim. Acta 51 (2006) 5508.
[14] M. Yoshio, Y. Xia, N. Kumada, S. Ma, J. Power Sources 101 (2001) 79.
[15] B. He, S. Bao, Y. Liang, J. Solid State Chem. 178 (2005) 897–901.
[16] N.V. Kosova, N.F. Uvarov, E.T. Devyatkina, Solid State Ionics 135 (2000) 107.
[17] K.S. Lee, S.T. Myung, H.J. Bang, S. Chung, Y.K. Sun, Electrochim. Acta 52 (2007) 5201.
[18] I. Tanifuchi, N. Fukuda, M. konarova, Powder Technol. 181 (2008) 228.